



# LUND UNIVERSITY

## The dual specificity PI3K/mTOR inhibitor PKI-587 displays efficacy against T-cell acute lymphoblastic leukemia (T-ALL)

Mohiuddin, Gazi; Moharram, Sausan A.; Marhäll, Alissa; Kazi, Julhash U.

*Published in:*  
Cancer Letters

*DOI:*  
[10.1016/j.canlet.2017.01.035](https://doi.org/10.1016/j.canlet.2017.01.035)

2017

*Document Version:*  
Peer reviewed version (aka post-print)

[Link to publication](#)

*Citation for published version (APA):*  
Mohiuddin, G., Moharram, S. A., Marhäll, A., & Kazi, J. U. (2017). The dual specificity PI3K/mTOR inhibitor PKI-587 displays efficacy against T-cell acute lymphoblastic leukemia (T-ALL). *Cancer Letters*, 392, 9-16.  
<https://doi.org/10.1016/j.canlet.2017.01.035>

*Total number of authors:*  
4

*Creative Commons License:*  
CC BY-NC-ND

### General rights

Unless other specific re-use rights are stated the following general rights apply:  
Copyright and moral rights for the publications made accessible in the public portal are retained by the authors and/or other copyright owners and it is a condition of accessing publications that users recognise and abide by the legal requirements associated with these rights.

- Users may download and print one copy of any publication from the public portal for the purpose of private study or research.
- You may not further distribute the material or use it for any profit-making activity or commercial gain
- You may freely distribute the URL identifying the publication in the public portal

Read more about Creative commons licenses: <https://creativecommons.org/licenses/>

### Take down policy

If you believe that this document breaches copyright please contact us providing details, and we will remove access to the work immediately and investigate your claim.

LUND UNIVERSITY

PO Box 117  
221 00 Lund  
+46 46-222 00 00

1 **The dual specificity PI3K/mTOR inhibitor PKI-587 displays efficacy against T-cell**  
2 **acute lymphoblastic leukemia (T-ALL)**

3

4 Mohiuddin Gazi<sup>1,2</sup>, Sausan A. Moharram<sup>1,2</sup>, Alissa Marhäll<sup>1,2</sup> and Julhash U. Kazi<sup>1,2\*</sup>

5

6 <sup>1</sup>Division of Translational Cancer Research, Department of Laboratory Medicine, Lund  
7 University, Lund, Sweden

8 <sup>2</sup>Lund Stem Cell Center, Department of Laboratory Medicine, Lund University, Lund,  
9 Sweden

10

11

12

13

14

15 **\*Corresponding authors:**

16 Julhash U. Kazi (kazi.uddin@med.lu.se)

17 Division of Translational Cancer Research

18 Department of Laboratory Medicine

19 Lund University, Medicon Village 404:C3

20 Scheelevägen 8, 22363 Lund, Sweden

21

22

23

24 **Abstract**

25 Although significant improvements have been made in the treatment of acute lymphoblastic  
26 leukemia (ALL), there is a substantial subset of high-risk T-cell ALL (T-ALL) patients with  
27 relatively poor prognosis. Like in other leukemia types, alterations of the PI3K/mTOR  
28 pathway are predominant in ALL which is also responsible for treatment failure and relapse.  
29 In this study, we show that relapsed T-ALL patients display an enrichment of the  
30 PI3K/mTOR pathway. Using a panel of inhibitors targeting multiple components of the  
31 PI3K/mTOR pathway, we observed that the dual-specific PI3K/mTOR inhibitor PKI-587 was  
32 the most selective inhibitor for T-ALL cells dependent on the PI3K/mTOR pathway.  
33 Furthermore, we observed that PKI-587 blocked proliferation and colony formation of T-ALL  
34 cell lines. Additionally, PKI-587 selectively abrogated PI3K/mTOR signaling without  
35 affecting MAPK signaling both in *in vitro* and *in vivo*. Inhibition of the PI3K/mTOR pathway  
36 using PKI-587 delayed tumor progression, reduced tumor load and enhanced the survival rate  
37 in immune-deficient mouse xenograft models without inducing weight loss in the inhibitor  
38 treated mice. This preclinical study shows beneficial effects of PKI-587 on T-ALL that  
39 warrants further investigation in the clinical setting.

40

41 **HIGHLIGHTS**

- 42       ➤ Pediatric relapsed T-ALL patients display upregulation of PI3K/mTOR pathway.
- 43       ➤ The dual specificity PI3K/mTOR inhibitor PKI-587 is a potent inhibitor of T-ALL
- 44       cells growth.
- 45       ➤ The dual specificity PI3K/mTOR inhibitor PKI-587 inhibited *in vitro* colony
- 46       formation.
- 47       ➤ PKI-587 delayed tumor formation and extended survival in a T-ALL xenograft model.
- 48       ➤ PKI-587 is a selective inhibitor of the PI3K/mTOR pathway both *in vitro* and *in vivo*.

49

50 **Keywords:** Leukemia; PI3K/mTOR; Gedatolisib; PF 05212384; T-ALL

51

52

53

54

55

56

57

## 58 INTRODUCTION

59 Acute lymphoblastic leukemia (ALL) is a neoplasm of immature lymphoid progenitors. ALL  
60 is the most common form of childhood leukemia that accounts for almost 30% of all  
61 childhood cancers [1]. T-cell acute lymphoblastic leukemia (T-ALL) is a subset of ALL  
62 affecting lymphoblast of the T-cell lineage. T-ALL represents for 15% of pediatric and 25%  
63 of adult ALL cases [2]. With risk-oriented chemotherapy and supportive care, 70-80% of  
64 children and 40% of adult ALL patients can reach long-term remission [3]. Despite significant  
65 improvements in cure rates, the survival of T-ALL patients with chemoresistant or relapsed  
66 leukemia is still very low [4]. This is mainly due to the insufficient understanding of T-ALL  
67 biology which may impede the identification of suitable prognostic factors for proper delivery  
68 of treatment.

69 Inhibitors of PI3K/mTOR pathway components have shown promising results in different  
70 cancers including hematological malignancies. Initially, rapamycin and its analogs were used  
71 for ALL treatment. Activation of PI3K/AKT pathway has been detected in 85% of T-ALL  
72 patients [5]. Since mTORC1 is a signaling molecule downstream of AKT, the initial treatment  
73 of T-ALL with rapamycin was logical. However, several feedback mechanisms are involved  
74 in the PI3K/mTOR signaling pathway [6]. Therefore, inhibitors targeting a single component  
75 of the pathway might not block oncogenic survival signaling. For example, activation of  
76 p70S6K by mTORC1 induces insulin receptor substrate-1 (IRS-1) phosphorylation and,  
77 thereby, dissociation of IRS-1 from its receptor. mTORC1 also phosphorylates GRB10 which  
78 leads to suppression of insulin signaling [7]. Furthermore, assembly of the mTORC2 complex  
79 is prevented by p70S6K-mediated phosphorylation of SIN1. Therefore, inhibition of  
80 mTORC1 by rapamycin (mTORC2 is insensitive to transient rapamycin treatment) can  
81 potentiate PI3K/AKT activation by removing a negative feedback control. Inhibition of both  
82 complexes through mTOR-specific inhibitors potently reduces AKT Ser<sup>473</sup> phosphorylation

83 but, due to the feedback loop, Thr<sup>308</sup> phosphorylation mediated by PDK1 is enhanced. Thus,  
84 an inhibitor with dual specificity against PI3K and mTOR provides better inhibitory capacity  
85 compared to targeting a single component of this pathway [8].

86 Advances in the structural and biochemical understanding of PI3K enzymes have over the last  
87 few decades enabled the development of various targeted inhibitors of the PI3K/AKT/mTOR  
88 pathway [9]. The Wyeth PI3K inhibitor discovery project identified an outstanding potent,  
89 selective, ATP-competitive, and reversible PI3K/mTOR inhibitor, PKI-587, for clinical  
90 development [10]. Preclinical data suggest its utility in the treatment of cancers with elevated  
91 PI3K/mTOR signaling and it has already exhibited effective antitumor activities against  
92 several cancers including breast, colon, glioma, and non-small cell lung cancer in *in vivo*  
93 xenograft models, which places it among the most potent dual specificity PI3K/mTOR  
94 inhibitors reported to date [11].

95 In this study, we analyzed the preclinical efficacy and therapeutic potential of PKI-587 on T-  
96 ALL cell line *in vitro* and on an *in vivo* mouse model. We observed strong cytotoxic activity  
97 against T-ALL cell lines and inhibition of PI3K/mTOR delayed tumor progression, reduced  
98 tumor volume and prolonged survival in a T-ALL xenograft mouse model.

99

## 100 **MATERIALS AND METHODS**

101 **Reagents, antibodies and inhibitors:** Horseradish peroxidase (HRP)-coupled secondary  
102 anti-mouse and anti-rabbit antibodies were from Thermo Fisher Scientific (Waltham, MA).  
103 Rabbit anti-phospho-AKT (pSer473), rabbit anti-phospho-ERK1/2 (pThr202/pThr204), goat  
104 anti-AKT, rabbit anti-ERK2, anti-rabbit secondary and anti-goat secondary antibodies were  
105 from Santa Cruz Biotechnology (Dallas, TX). Mouse anti-phospho-p38 and anti-p38  
106 antibodies were from BD Transduction Laboratories (Franklin Lakes, NJ). All inhibitors were  
107 from Selleck Chemicals (Houston, TX).

108 **Drug preparation:** For *in vitro* studies, PKI-587 was dissolved in DMSO at 5 mM  
109 concentration and stored at -80°C. Before starting the experiments, aliquots were thawed and  
110 diluted to the desired concentrations in the corresponding medium. In the case of *in vivo*  
111 studies, PKI-587 was dissolved in vehicle (5% dextrose in water and 0.3% lactic acid, pH  
112 3.5). Freshly prepared inhibitor solutions were always used in both the *in vitro* and *in vivo*  
113 experiments.

114 **Cell culture:** All cell lines were obtained from Deutsche Sammlung von Mikroorganismen  
115 und Zellkulturen (DSMZ, Braunschweig, Germany). CCRF-CEM, MOLT3, and Jurkat cells  
116 were maintained in RPMI 1640 medium supplemented with 10% heat-inactivated FBS, 100  
117 units/ml penicillin and 100µg/ml streptomycin.

118 **Cell lysis and western blotting:** CCRF-CEM and MOLT3 cells were washed with cold PBS  
119 and then treated with increased concentrations of PKI-587 for 4 hours in RPMI-1640. Cells  
120 were then washed and lysed in 1% Triton X-100 lysis buffer. The Western blotting and  
121 immunodetection procedures were described earlier [12].

122 **Cell viability:** CCRF-CEM and MOLT3 cells grown in RPMI 1640 supplemented with 10%  
123 FBS, 100 units/ml penicillin and 100 µg/ml streptomycin. Cells were then seeded in 96-well  
124 plates (13,000 cells per well). Two days after seeding, cell viability was counted by  
125 PrestoBlue (Molecular Probes, Eugene, OR) assay.

126 **Apoptosis:** CCRF-CEM and MOLT-3 cells were washed and seeded in 12-well plates  
127 (100,000 cells per well) with increasing concentrations of PKI-587. Two days after seeding,  
128 apoptosis was measured by flow cytometry using Annexin V and 7-aminoactinomycin D (7-  
129 AAD) apoptosis kit (BD Biosciences, Franklin Lakes, NJ).

130 **Peptide-based kinase profiling:** PamGene technology (PamGene, 's-Hertogenbosch, the  
131 Netherlands) was used to measure kinase activity of T-ALL cells. Cells were serum-starved  
132 overnight before lysis. Five micrograms of total protein were used for tyrosine kinase

133 profiling and 0.5  $\mu$ g of total protein was used for serine/threonine kinase profiling using  
134 standard protocol provided by PamGene.

135 **Colony formation assay:** CCRF-CEM and MOLT3 cells were washed with IMDM and 600  
136 cells were mixed with 500  $\mu$ l of 80% methylcellulose medium and 20% IMDM. Cells were  
137 seeded in 24-well plates with increasing concentrations (0-50 nM) of PKI-587 and incubated  
138 for 7 days. After seven-day colonies were visible to the eye and counted by two individual  
139 researchers. Picture of each well was taken by using a light microscope.

140 **Xenograft studies:** Ten female NOD/SCID nude mice each weighing approximately 20g,  
141 (housed by the Laboratory Animal Facilities at Medicon Village, Lund University) were  
142 injected subcutaneously with 2 million cells. Mice were then divided into two groups that  
143 were either treated with PKI-587 or vehicle. One week after injection of cells, mice were  
144 treated twice weekly by intravenous injection of 12 mg/kg PKI-587 or vehicle for additional  
145 20 days. Drug efficacy was monitored by checking the tumor growth in both groups and by  
146 measuring the body weight of the mice regularly. After the size of the tumors had reached  
147 about 1 cm<sup>3</sup>, mice were sacrificed. For analysis of signaling proteins, tumors excised and  
148 rapidly transferred to liquid nitrogen. Another group of female NOD/SCID nude mice were  
149 injected intravenously through the tail vein with 1 million cells and divided into two groups  
150 that were either treated with PKI-587 or vehicle. Ten days after injection of cells, treatment of  
151 mice was commenced by intravenous injection of 12 mg/kg of PKI-587 or vehicle twice  
152 weekly. Engraftment was checked by measuring the number of circulating CD45+ cells. Mice  
153 were euthanized when any signs of suffering such as difficulty in breathing, lack of  
154 movement, or paralysis observed. All animal experiments were performed under an ethical  
155 permit from the Swedish Animal Welfare Authority.

156 **Statistical analysis:** Statistical analysis was performed using GraphPad Prism 5.0. One way  
157 ANOVA was used where needed.



158

## 159 **RESULTS**

### 160 **Pediatric relapsed acute lymphoblastic leukemia patients display an enrichment of the**

### 161 **PI3K/mTOR pathway:**

162 To determine the dependency of the signaling pathways in T-ALL cells, we analyzed two  
163 different gene expression datasets (GSE13576 and GSE14618) from T-ALL patients. We  
164 compared gene set enrichment using GSEA between one group of patients that relapsed after  
165 treatment and one that got complete remission [13-15]. We observed that patients who had  
166 relapsed during disease progression displayed an enrichment of the PI3K/mTOR pathway  
167 (Fig. 1A and 1B). To follow up on the GSEA results, we used the patient-derived T-ALL cell  
168 lines Jurkat, MOLT3 and CCRF-CEM. All three cell lines displayed strong activation of the  
169 PI3K/mTOR pathway as we observed constitutive phosphorylation of AKT-Ser-473, AKT-  
170 Thr-308 and S6K-Thr-389 (Fig. 1C). Additionally, Jurkat cells show strong activation of the  
171 ERK pathway (Fig. 1D). Thus, it is likely that while MOLT3 and CCRF-CEM cells are  
172 dependent on the PI3K/mTOR pathway, Jurkat cells utilize additional survival signaling  
173 pathways. Furthermore, peptide-based kinase profiling assays suggested that while S6K was  
174 highly activated in MOLT3 cells, many tyrosine kinases were active in Jurkat cells (Fig. 2).

175

### 176 **The dual PI3K/mTOR inhibitor PKI-587 is a potent inhibitor of T-ALL cells growth:**

177 Since we observed that relapsed ALL patients display upregulation of the PI3K/mTOR  
178 pathway, we decided to use a panel of inhibitors that target different components of the  
179 PI3K/mTOR pathway. We used 88 different inhibitors targeting AKT, AMPK, ATM/ATR,  
180 ATM/ATR and mTOR, GSK-3, mTOR, PDK-1, PI3K, PI3K and DNA-PK, PI3K, mTOR,  
181 PKA and S6K. As Jurkat cells display upregulation of both the PI3K/mTOR and MAPK  
182 pathways, we speculated that selective PI3K/mTOR pathway inhibitors would not block the

183 cell viability of Jurkat cells and thus could be used as a control. We compared cell viability  
184 between Jurkat and CCRF-CEM cells in the presence of 88 different inhibitors in two  
185 different concentrations, 100 nM (Fig. 3A) and 1000 nM (Fig. 3B). We observed that while  
186 most of the inhibitors displayed a linear correlation between the two cell lines, PKI-587 was  
187 the most selective inhibitor for CCRF-CEM cells. Additionally, PKI-587 displayed an IC<sub>50</sub> of  
188 25 nM for MOLT3 cells (Fig. 3C), 23 nM for CCRF-CEM cells (Fig. 3D) and 73 nM for  
189 Jurkat cells (Fig. 3E).

190

191 **Cytokines secreted from bone marrow HS-5 cells have no effect on inhibition of cell**  
192 **growth by PKI-587:**

193 Cytokines/chemokines/growth factors secreted by the bone marrow microenvironment can  
194 drive the drug resistance and survival of leukemic blasts [16]. In order to investigate whether  
195 PKI-587 can still efficiently block cell growth in the presence of micro-environmental factors,  
196 we assessed the relative viability of MOLT3 and CCRF-CEM cells in the presence or absence  
197 of conditioned medium from HS5 cell cultures with increasing concentrations of inhibitor.  
198 We observed that the presence or absence of conditioned medium from HS5 cells did not  
199 affect the ability of PKI-587 to induce growth inhibition in MOLT3 (Fig. 4A) and CCRF-  
200 CEM (Fig. 4B) cells.

201

202 **The dual specificity PI3K/mTOR inhibitor PKI-587 reduces viability and colony**  
203 **formation of T-ALL cells:**

204 We used different biological assays to evaluate the effect PKI-587 on T-ALL cells. We  
205 observed a dose-dependent inhibition of cell growth of both MOLT3 (Fig. 5A) and CCRF-  
206 CEM (Fig. 5B) cell lines. Colony formation assays in semi-solid medium also indicated a  
207 marked decrease in the number of colonies (Fig. 5C and 5D) as well as the size of the

208 colonies (Fig. 5E and 5F) with the increasing concentration of PKI-587 on both MOLT3 and  
209 CCRF-CEM cells. Additionally, treatment with PKI-587 induced apoptosis in a dose-  
210 dependent manner in these cell lines (data not shown). These results demonstrate an effective  
211 inhibitory action of PKI-587 on T-ALL cell lines.

212

### 213 **PKI-587 delays tumor formation and extended survival in T-ALL xenograft models:**

214 Based on the potent inhibitory efficacy of PKI-587 on the PI3K/mTOR pathway in T-ALL  
215 cell lines *in vitro*, we next assessed its therapeutic efficacy in preclinical mouse models. We  
216 first developed a mouse xenograft model using immunodeficient mice. We subcutaneously  
217 injected only CCRF-CEM cells since it has been reported that MOLT3 cells are unable to  
218 induce tumors *in vivo* by themselves [17]. Seven days after cell injection, mice were treated  
219 with 12 mg/kg body weight of PKI-587, or vehicle, for an additional 20 days. Treatment with  
220 PKI-587 led to a marked inhibition of tumor growth compared to vehicle treatment (Fig. 6A),  
221 as well as to a delay in tumor growth in all treated mice (Fig. 6B). This three-week treatment  
222 regimen also led to a significant tumor regression in the treated group (Fig. 6C). To assess the  
223 survival benefit of this drug, we further developed a mouse model where we injected CCRF-  
224 CEM cells intravenously. Ten days after the cells were injected, mice were treated with 12  
225 mg/kg body weight of PKI-587 or vehicle control. Since CD45+ cells in the blood circulation  
226 indicate the presence of leukocytes and engraftment of the injected cells, we measured those  
227 cells in blood circulation in both mice treated with PKI-587 and vehicle controls. As  
228 expected, the mice treated with PKI-587 exhibited significantly lower numbers of CD45+  
229 cells in the blood circulation compared to the vehicle-treated (control) group (Fig. 6D). The  
230 untreated first mouse was euthanized on day 40 with a median survival of 45 days, while PKI-  
231 587-treatment led to a significantly higher survival advantage (Fig. 6E). The effects of this *in*  
232 *vivo* treatment were well tolerated since no deceptive decrease in body weight was noticed in

233 the treated animals (data not shown). To summarize, these *in vivo* data indicate that PKI-587  
234 has a substantial preclinical efficacy in treating T-ALL and warrants further investigation in a  
235 clinical setting.

236

237 **PKI-587 is a selective inhibitor of the PI3K/mTOR pathway both *in vitro* and *in vivo*:**

238 It is a common phenomenon for oncogenic signaling network to exhibit crosstalk between  
239 multiple cellular signaling pathways. This has sometimes led to wrong interpretation and  
240 overestimation of the role of a single protein in response to drug treatment [18]. PKI-587 has  
241 already been shown to be a highly selective inhibitor of the PI3K/mTOR pathway in several  
242 cancer types [10] and has been studied in different cell models, animal models and in clinical  
243 trials [19, 20]. On the basis of the previous reports and our preliminary data, we further  
244 evaluated the effect of PKI-587 on other signaling pathways. While treating the cells with a  
245 higher concentration of PKI-587, we observed decreased phosphorylation of AKT and S6K  
246 but no effect on ERK1/2 and p38 phosphorylation *in vitro* (Fig. 7A). Similar to the *in vitro*  
247 findings, PKI-587 selectively inhibited AKT and S6K phosphorylation *in vivo* (Fig. 7B).  
248 These results strongly suggest that PKI-587 is a selective inhibitor of the PI3K/mTOR  
249 pathway.

250

251 **DISCUSSION**

252 Although significant improvement has been observed in overall cure rates of ALL, the  
253 outcome of relapsed T-ALL patients still remains a major clinical challenge. This can be  
254 attributed to several factors, but it is mainly due to the insufficient understanding of T-ALL  
255 biology which impedes the identification of suitable prognostic factors to deliver proper  
256 treatment. With the improved cure rate in ALL, current research strategies are more focused

257 on subsets of patients such as T-ALL with drug resistance or relapsed leukemia in order to  
258 identify treatments with the effective outcome.

259 The PI3K/mTOR pathway plays a critical role in T-ALL pathogenesis since the most  
260 common mutations in T-ALL, such as gain-of-function mutations of NOTCH1 or loss-of-  
261 function mutation of PTEN, often cause constitutive activation of this pathway [21]. In this  
262 study, two different gene expression datasets of relapsed patients also displayed a  
263 predominant enrichment of the PI3K/mTOR pathway. Using a panel of 88 different inhibitors  
264 which target several different components of this pathway, PKI-587 was found to be the most  
265 selective drug that induces apoptosis of T-ALL cell lines that are dependent on the activity of  
266 the PI3K/mTOR pathway. An important observation was made, that the inhibitor PKI-587  
267 was effective even in the presence of micro-environmental factors. The use of conditioned  
268 medium from the bone marrow HS5 cells had very little or no effect on PKI-587-induced  
269 inhibition of cell growth. This is interesting since it has been suggested that the bone marrow  
270 microenvironment, presumably through cytokine production, helps to protect leukemic cells  
271 from drug-induced death and thereby contributes to therapy resistance. Our findings provide  
272 a basis for the use of the dual specificity inhibitor PKI-587 as a promising drug for the  
273 treatment of T-ALL. Our biological assays also suggest a strong ability of PKI-578 to block  
274 cell proliferation, colony formation and to induce apoptosis of T-ALL cell lines.

275

276 Since PKI-587 is a potent ATP-competitive, and reversible PI3K/mTOR inhibitor, it can  
277 selectively abrogate the PI3K/mTOR pathway, without affecting MAPK signaling, by  
278 inhibiting the activity of PI3K and mTOR along with their downstream effectors AKT and  
279 S6K both *in vitro* as well as *in vivo*. Our results are in line with previous findings, in a slightly  
280 different context, on the signaling effects of this dual inhibitor on therapy-resistant AML  
281 patient with FLT3-ITD mutation [22]. In xenograft models of the T-ALL cell, inhibition of

282 the PI3K/mTOR pathway led to delayed tumor progression, induction of tumor regression and  
283 markedly increased the survival rate. No gross toxicity was observed as no deceptive  
284 decrease of body weight was noticed in tumor-bearing or engrafted mice. Our conclusion is  
285 that this dose is effective and well tolerated, suggesting an encouraging therapeutic window  
286 for the treatment of relapsed T-ALL patients.

287 In conclusion, we have investigated the beneficial effects of the dual PI3K/mTOR inhibitor  
288 PKI-587, both *in vitro* and *in vivo*, for the treatment of relapsed and therapy-resistant T-ALL.  
289 Our study has dominantly revealed a preclinical rationale to explore this novel drug to  
290 effectively inhibit PI3K/mTOR activated signaling pathway. However, observations of the  
291 pathway enrichment and the method to block the signaling pathway with PKI-587 may be a  
292 possible therapeutic way to treat relapsed T-ALL patients and thereby minimizing the diverse  
293 effects. Since this drug is already in clinical trials for the treatment of other cancers, we  
294 suggest that further pre-clinical trials and early phase clinical trial should be undertaken to  
295 evaluate the effect of PKI-587 on patients with relapsed T-ALL.

296

297

#### 298 **Acknowledgments:**

299 We thank Professor Lars Rönstrand for kind support and critical comments on the  
300 manuscript. This research was funded by Kungliga Fysiografiska Sällskapet i Lund, Per-Eric  
301 och Ulla Schybergs stiftelse, Ollie and Elof Ericssons Stiftelse, Stiftelsen Thelma Zoégas, the  
302 Crafoord Foundation, Stiftelsen Clas Groschinskys Minnesfond and the Swedish Childhood  
303 Cancer Foundation. JUK is a recipient of an Assistant Professorship (forskarassistenttjänst)  
304 grant from the Swedish Childhood Cancer Foundation.

305

#### 306 **Conflict of interest:**

307 The authors declare no conflict of interest.

308

## 309 REFERENCES

- 310 [1] R. Siegel, D. Naishadham, A. Jemal, Cancer statistics, 2013, *CA Cancer J Clin*, 63 (2013)  
311 11-30.
- 312 [2] A. Lonetti, A. Cappellini, A. Bertaina, F. Locatelli, A. Pession, F. Buontempo, C.  
313 Evangelisti, C. Evangelisti, E. Orsini, L. Zambonin, L.M. Neri, A.M. Martelli, F. Chiarini,  
314 Improving nelarabine efficacy in T cell acute lymphoblastic leukemia by targeting aberrant  
315 PI3K/AKT/mTOR signaling pathway, *J Hematol Oncol*, 9 (2016) 114.
- 316 [3] M.D. Kraszewska, M. Dawidowska, T. Szczepanski, M. Witt, T-cell acute lymphoblastic  
317 leukaemia: recent molecular biology findings, *Br J Haematol*, 156 (2012) 303-315.
- 318 [4] P. Van Vlierberghe, A. Ferrando, The molecular basis of T cell acute lymphoblastic  
319 leukemia, *J Clin Invest*, 122 (2012) 3398-3406.
- 320 [5] A. Silva, J.A. Yunes, B.A. Cardoso, L.R. Martins, P.Y. Jotta, M. Abecasis, A.E. Nowill,  
321 N.R. Leslie, A.A. Cardoso, J.T. Barata, PTEN posttranslational inactivation and  
322 hyperactivation of the PI3K/Akt pathway sustain primary T cell leukemia viability, *J Clin*  
323 *Invest*, 118 (2008) 3762-3774.
- 324 [6] E. Rozengurt, H.P. Soares, J. Sinnet-Smith, Suppression of feedback loops mediated by  
325 PI3K/mTOR induces multiple overactivation of compensatory pathways: an unintended  
326 consequence leading to drug resistance, *Mol Cancer Ther*, 13 (2014) 2477-2488.
- 327 [7] C.C. Dibble, L.C. Cantley, Regulation of mTORC1 by PI3K signaling, *Trends Cell Biol*,  
328 25 (2015) 545-555.
- 329 [8] C.P. Hall, C.P. Reynolds, M.H. Kang, Modulation of Glucocorticoid Resistance in  
330 Pediatric T-cell Acute Lymphoblastic Leukemia by Increasing BIM Expression with the  
331 PI3K/mTOR Inhibitor BEZ235, *Clin Cancer Res*, 22 (2016) 621-632.
- 332 [9] S.K. Tasian, D.T. Teachey, S.R. Rheingold, Targeting the PI3K/mTOR Pathway in  
333 Pediatric Hematologic Malignancies, *Front Oncol*, 4 (2014) 108.
- 334 [10] A.M. Venkatesan, C.M. Dehnhardt, E. Delos Santos, Z. Chen, O. Dos Santos, S. Ayril-  
335 Kaloustian, G. Khafizova, N. Brooijmans, R. Mallon, I. Hollander, L. Feldberg, J. Lucas, K.  
336 Yu, J. Gibbons, R.T. Abraham, I. Chaudhary, T.S. Mansour, Bis(morpholino-1,3,5-triazine)  
337 derivatives: potent adenosine 5'-triphosphate competitive phosphatidylinositol-3-  
338 kinase/mammalian target of rapamycin inhibitors: discovery of compound 26 (PKI-587), a  
339 highly efficacious dual inhibitor, *J Med Chem*, 53 (2010) 2636-2645.
- 340 [11] R. Mallon, L.R. Feldberg, J. Lucas, I. Chaudhary, C. Dehnhardt, E.D. Santos, Z. Chen,  
341 O. dos Santos, S. Ayril-Kaloustian, A. Venkatesan, I. Hollander, Antitumor efficacy of PKI-  
342 587, a highly potent dual PI3K/mTOR kinase inhibitor, *Clin Cancer Res*, 17 (2011) 3193-  
343 3203.
- 344 [12] S.A. Moharram, R.A. Chougule, X. Su, T. Li, J. Sun, H. Zhao, L. Rönnstrand, J.U. Kazi,  
345 Src-like adaptor protein 2 (SLAP2) binds to and inhibits FLT3 signaling, *Oncotarget*, (2016).
- 346 [13] A. Gutierrez, A. Kentsis, T. Sanda, L. Holmfeldt, S.C. Chen, J. Zhang, A. Protopopov, L.  
347 Chin, S.E. Dahlberg, D.S. Neuberg, L.B. Silverman, S.S. Winter, S.P. Hunger, S.E. Sallan, S.  
348 Zha, F.W. Alt, J.R. Downing, C.G. Mullighan, A.T. Look, The BCL11B tumor suppressor is  
349 mutated across the major molecular subtypes of T-cell acute lymphoblastic leukemia, *Blood*,  
350 118 (2011) 4169-4173.
- 351 [14] T. Sanda, X. Li, A. Gutierrez, Y. Ahn, D.S. Neuberg, J. O'Neil, P.R. Strack, C.G. Winter,  
352 S.S. Winter, R.S. Larson, H. von Boehmer, A.T. Look, Interconnecting molecular pathways

353 in the pathogenesis and drug sensitivity of T-cell acute lymphoblastic leukemia, *Blood*, 115  
354 (2010) 1735-1745.

355 [15] S.S. Winter, Z. Jiang, H.M. Khawaja, T. Griffin, M. Devidas, B.L. Asselin, R.S. Larson,  
356 G. Children's Oncology, Identification of genomic classifiers that distinguish induction failure  
357 in T-lineage acute lymphoblastic leukemia: a report from the Children's Oncology Group,  
358 *Blood*, 110 (2007) 1429-1438.

359 [16] F. Chiarini, A. Lonetti, C. Evangelisti, F. Buontempo, E. Orsini, C. Evangelisti, A.  
360 Cappellini, L.M. Neri, J.A. McCubrey, A.M. Martelli, Advances in understanding the acute  
361 lymphoblastic leukemia bone marrow microenvironment: From biology to therapeutic  
362 targeting, *Biochim Biophys Acta*, 1863 (2016) 449-463.

363 [17] S. Indraccolo, L. Stievano, S. Minuzzo, V. Tosello, G. Esposito, E. Piovan, R. Zamarchi,  
364 L. Chieco-Bianchi, A. Amadori, Interruption of tumor dormancy by a transient angiogenic  
365 burst within the tumor microenvironment, *Proc Natl Acad Sci U S A*, 103 (2006) 4216-4221.

366 [18] J.B. Fitzgerald, B. Schoeberl, U.B. Nielsen, P.K. Sorger, Systems biology and  
367 combination therapy in the quest for clinical efficacy, *Nat Chem Biol*, 2 (2006) 458-466.

368 [19] V. D'Amato, R. Rosa, C. D'Amato, L. Formisano, R. Marciano, L. Nappi, L. Raimondo,  
369 C. Di Mauro, A. Servetto, C. Fusciello, B.M. Veneziani, S. De Placido, R. Bianco, The dual  
370 PI3K/mTOR inhibitor PKI-587 enhances sensitivity to cetuximab in EGFR-resistant human  
371 head and neck cancer models, *Br J Cancer*, 110 (2014) 2887-2895.

372 [20] R. Gedaly, P. Angulo, J. Hundley, M.F. Daily, C. Chen, B.M. Evers, PKI-587 and  
373 sorafenib targeting PI3K/AKT/mTOR and Ras/Raf/MAPK pathways synergistically inhibit  
374 HCC cell proliferation, *J Surg Res*, 176 (2012) 542-548.

375 [21] T. Palomero, M.L. Sulis, M. Cortina, P.J. Real, K. Barnes, M. Ciofani, E. Caparros, J.  
376 Buteau, K. Brown, S.L. Perkins, G. Bhagat, A.M. Agarwal, G. Basso, M. Castillo, S. Nagase,  
377 C. Cordon-Cardo, R. Parsons, J.C. Zuniga-Pflucker, M. Dominguez, A.A. Ferrando,  
378 Mutational loss of PTEN induces resistance to NOTCH1 inhibition in T-cell leukemia, *Nat*  
379 *Med*, 13 (2007) 1203-1210.

380 [22] O. Lindblad, E. Cordero, A. Puissant, L. Macaulay, A. Ramos, N.N. Kabir, J. Sun, J.  
381 Vallon-Christersson, K. Haraldsson, M.T. Hemann, A. Borg, F. Levander, K. Stegmaier, K.  
382 Pietras, L. Rönstrand, J.U. Kazi, Aberrant activation of the PI3K/mTOR pathway promotes  
383 resistance to sorafenib in AML, *Oncogene*, 35 (2016) 5119-5131.

384

## 385 **FIGURE LEGENDS:**

386 **Figure 1:** T-ALL patients display upregulation of the PI3K/mTOR pathway: (A-B) Gene  
387 expression data from GSE13576 and GSE14618 were used for gene set enrichment analysis  
388 (GSEA). (C-D) Cell lysates from Jurkat, MOLT3 and CCRF-CEM were used to check  
389 phosphorylation of signaling proteins using phospho-specific antibodies.

390 **Figure 2:** Peptide-based kinase profiling shows upregulation of PI3K/mTOR pathway in  
391 MOLT3 cells. Kinome tree was generated using Kinome-render  
392 (<http://bcb.med.usherbrooke.ca/kinomerender.php>) online tool. Red: upregulated kinase  
393 activity in MOLT3 cells, Green: upregulated kinase activity in Jurkat cells.



394 **Figure 3:** PKI-587 is a potent inhibitor of T-ALL cells growth: (A-B) A panel of inhibitors  
395 (100 nM and 1000 nM concentrations) targeting different components of the PI3K/mTOR  
396 pathway was used to measure cell viability using PrestoBlue assay. (C-E). Cell viability was  
397 measured using PrestoBlue assay in the presence of increasing concentrations of PKI-587.

398 **Figure 4:** Conditioned medium from HS5 cells has no effect on PKI-587 induced growth  
399 inhibition: (A-B) Cells were treated with increasing concentration of PKI-587 in the presence  
400 or absence of conditioned medium from HS5 cells. PrestoBlue viability assay was used to  
401 measure cell viability.

402 **Figure 5:** PKI-587 reduces cell viability and colony formation: (A-B) Cells were treated with  
403 increasing concentrations of inhibitor. Cell viability was measured using PrestoBlue. (C-F)  
404 Cells were mixed with semi-solid medium and inhibitor and seeded in 24-well plates.  
405 Colonies were counted after 7 days. ns, not significant; \*\*\*,  $p < 0.001$ .

406 **Figure 6:** PKI-587 decreases tumor growth and increases survival: (A) Mice were treated  
407 with PKI-587 or vehicle. Tumor volume was measured twice a week. (B-C) Tumors were  
408 removed after sacrificing mice. The weight of individual tumors was measured, and the  
409 picture was taken in the presence of a scale. (D) CD45+ cells in blood were counted using an  
410 antibody against human CD45. (E) Kaplan–Meier curves showed the overall survival of mice  
411 transplanted with CCRF-CEM cells.

412 **Figure 7:** PKI-587 selectively inhibits AKT and S6K phosphorylation: (A) Cells were treated  
413 with increasing concentrations of PKI-587 before lysis. Cell lysates were used to assess  
414 phosphorylation of signaling proteins using phospho-specific antibodies. (B) Tumors from  
415 mice treated with either PKI-587 or vehicle were used to assess phosphorylation of signaling  
416 proteins using phospho-specific antibodies.

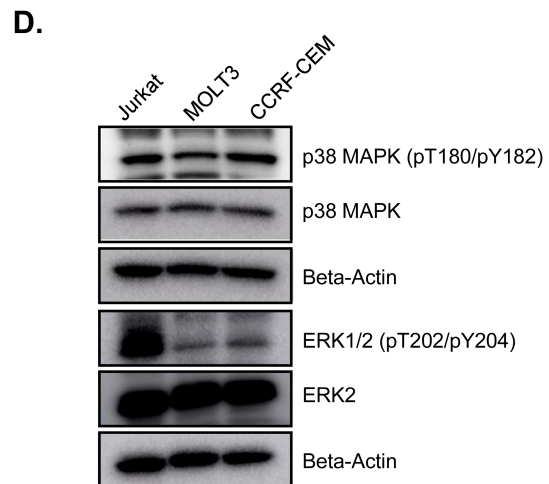
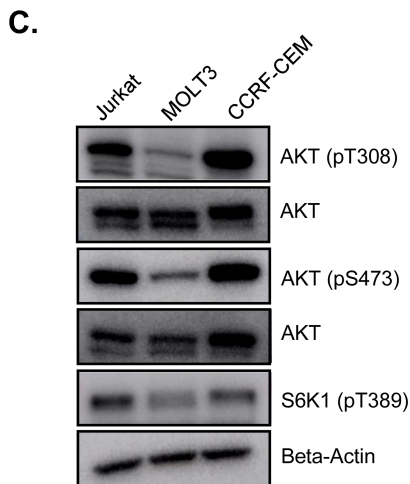
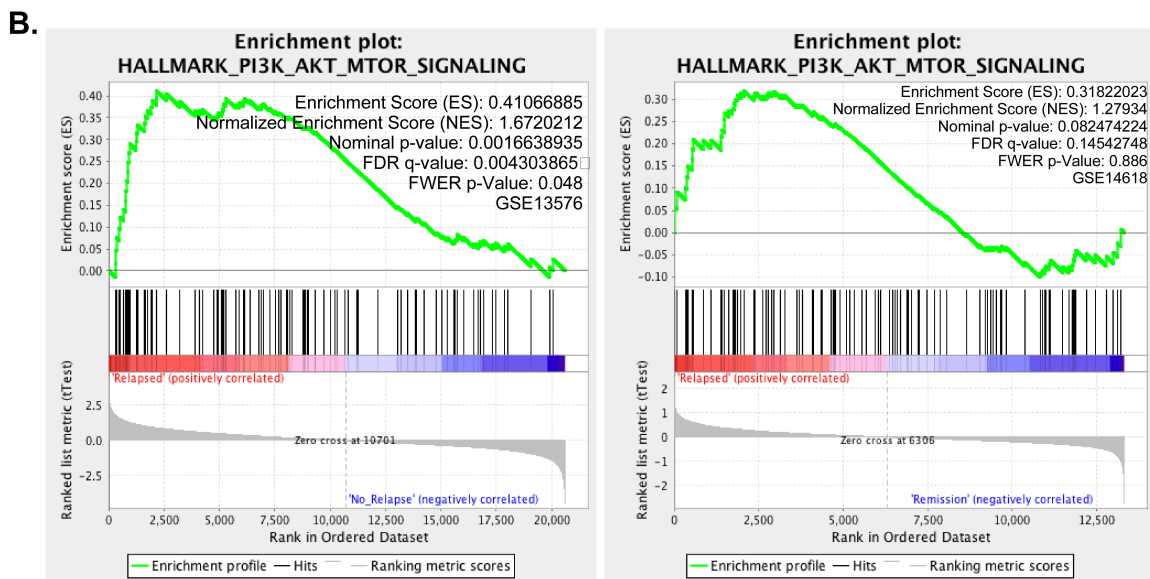
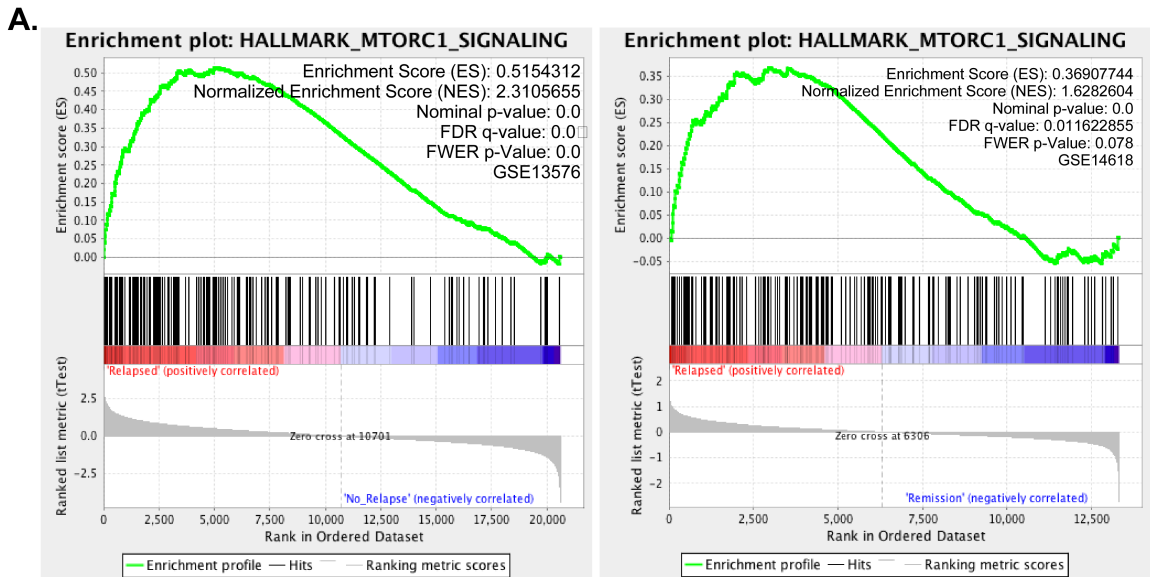
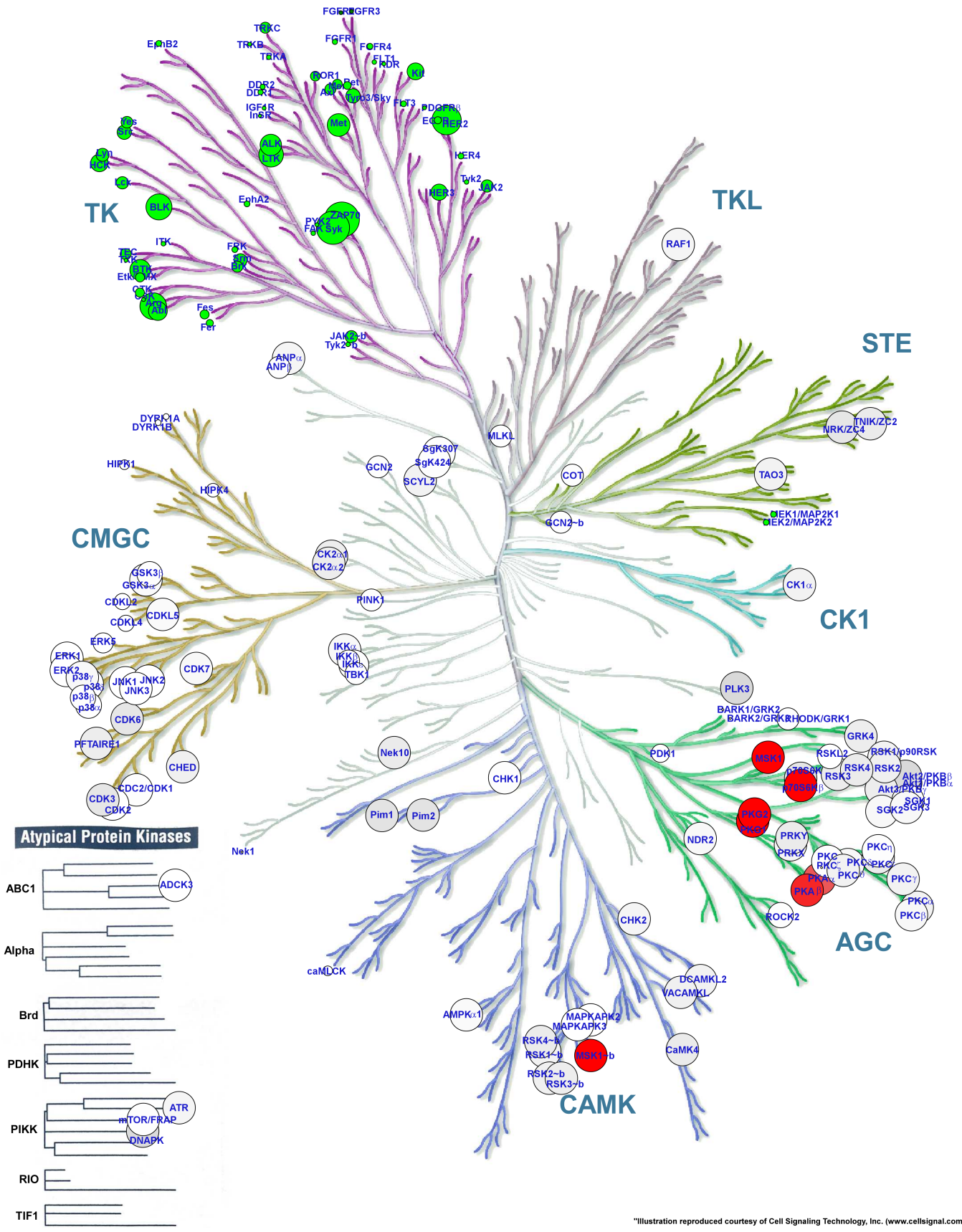


Figure 1



"Illustration reproduced courtesy of Cell Signaling Technology, Inc. ([www.cellsignal.com](http://www.cellsignal.com))"

Figure 2

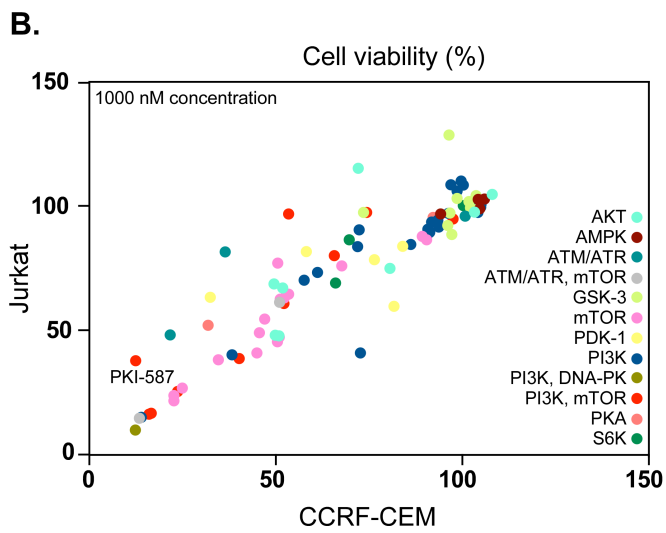
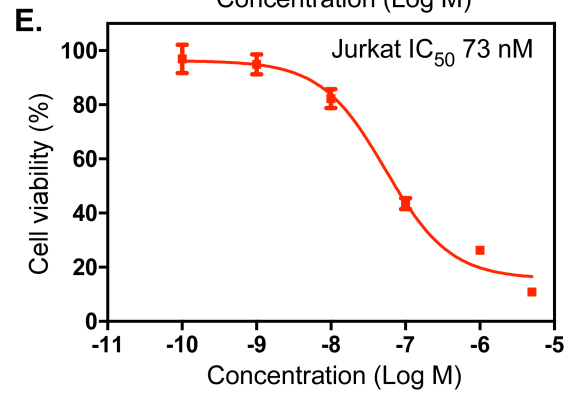
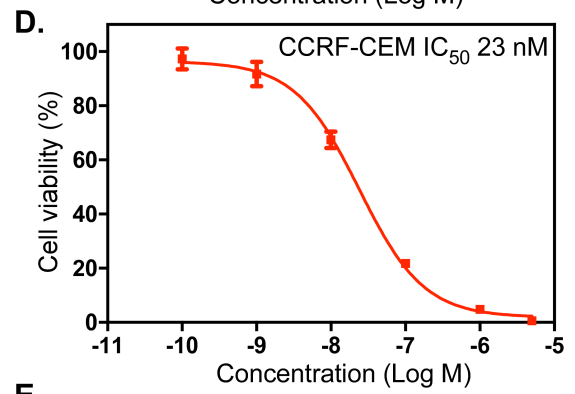
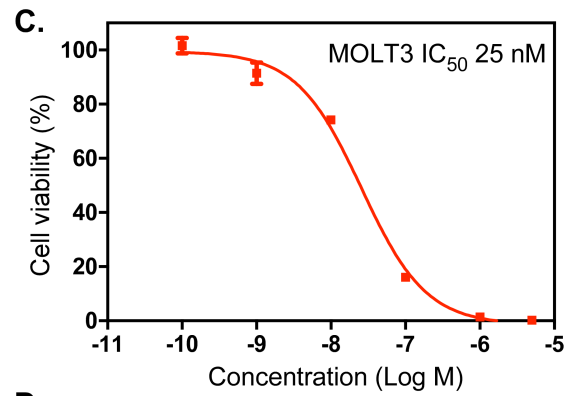
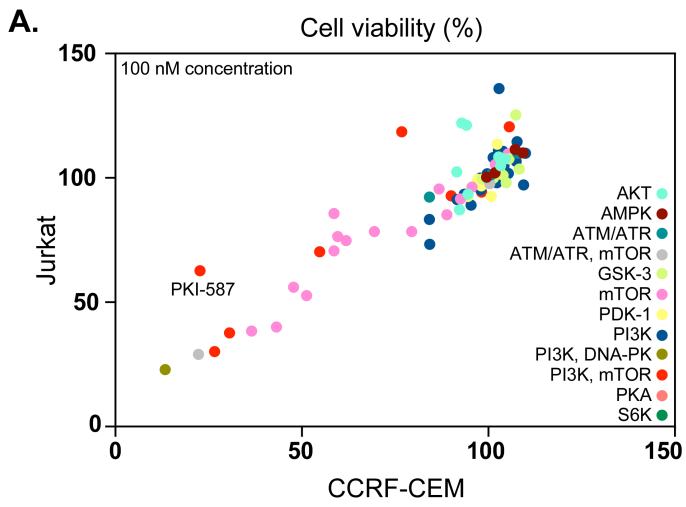


Figure 3

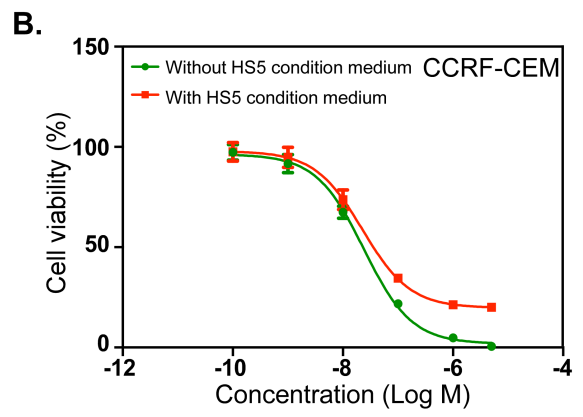
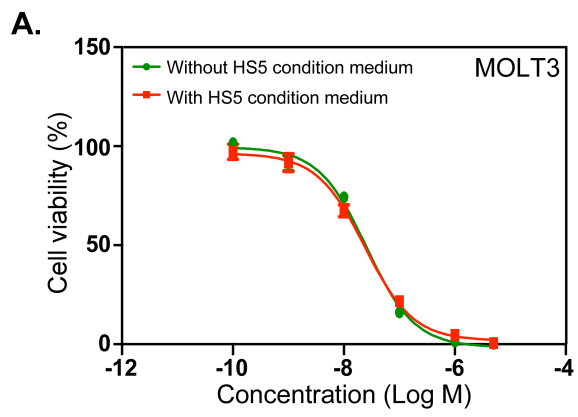


Figure 4

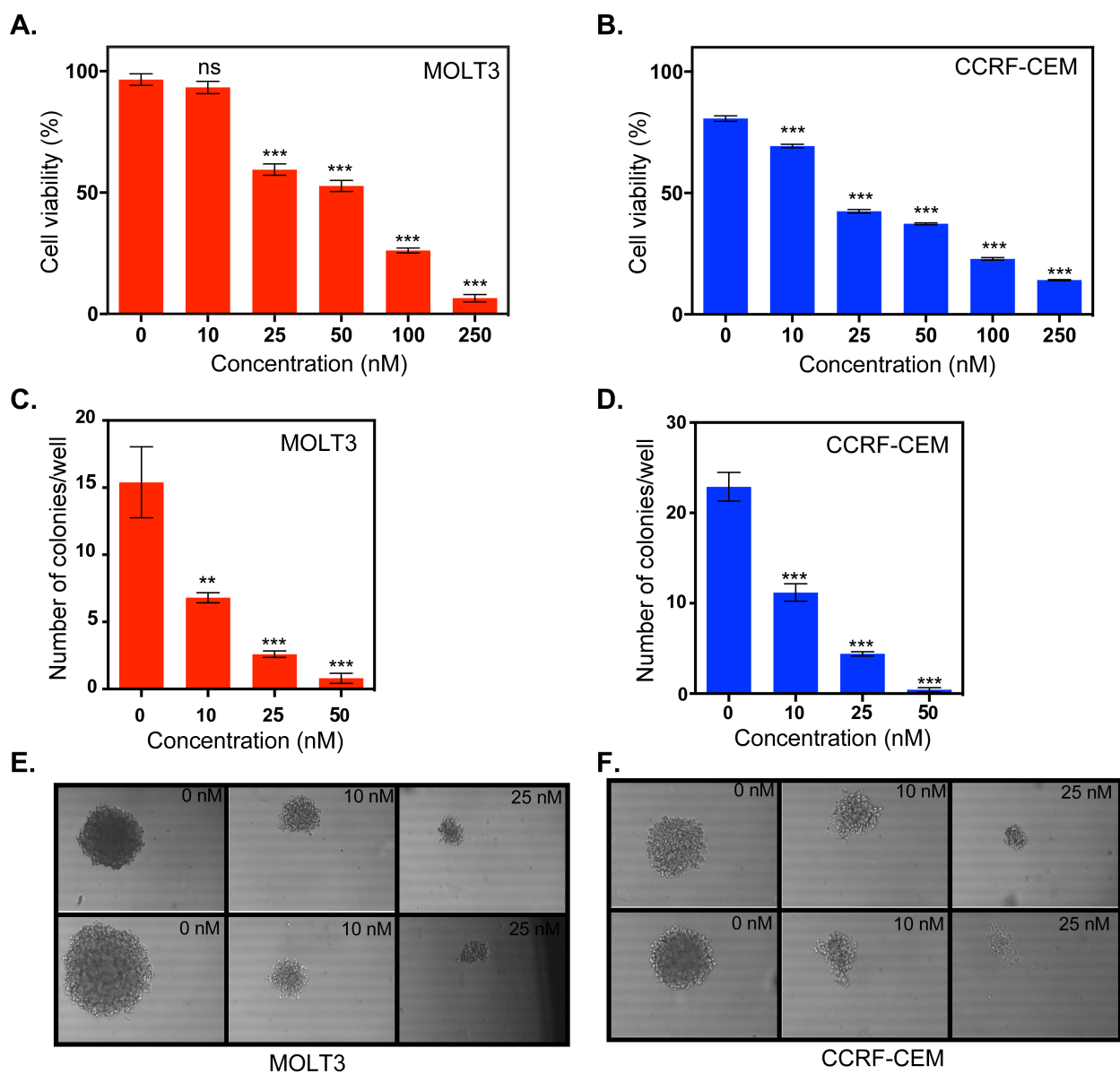


Figure 5

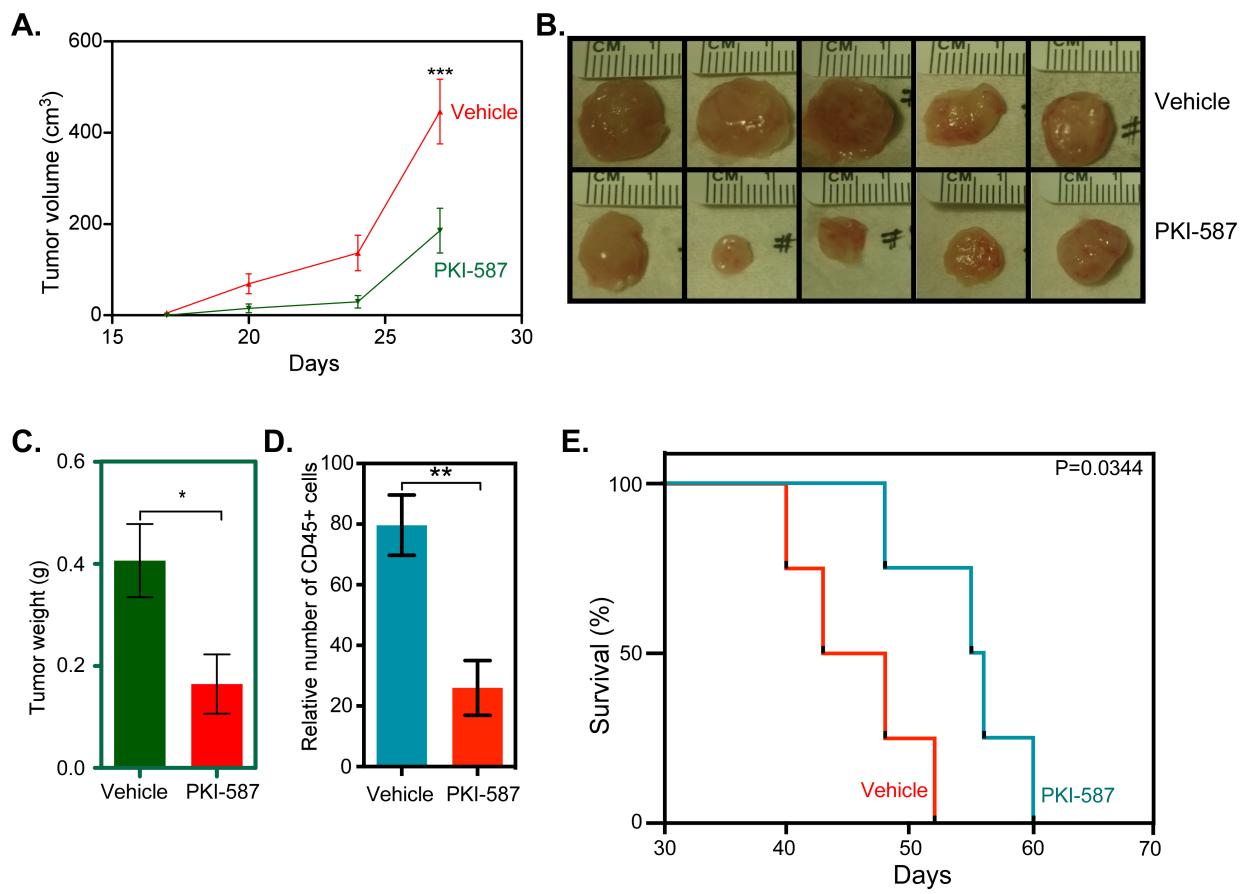


Figure 6

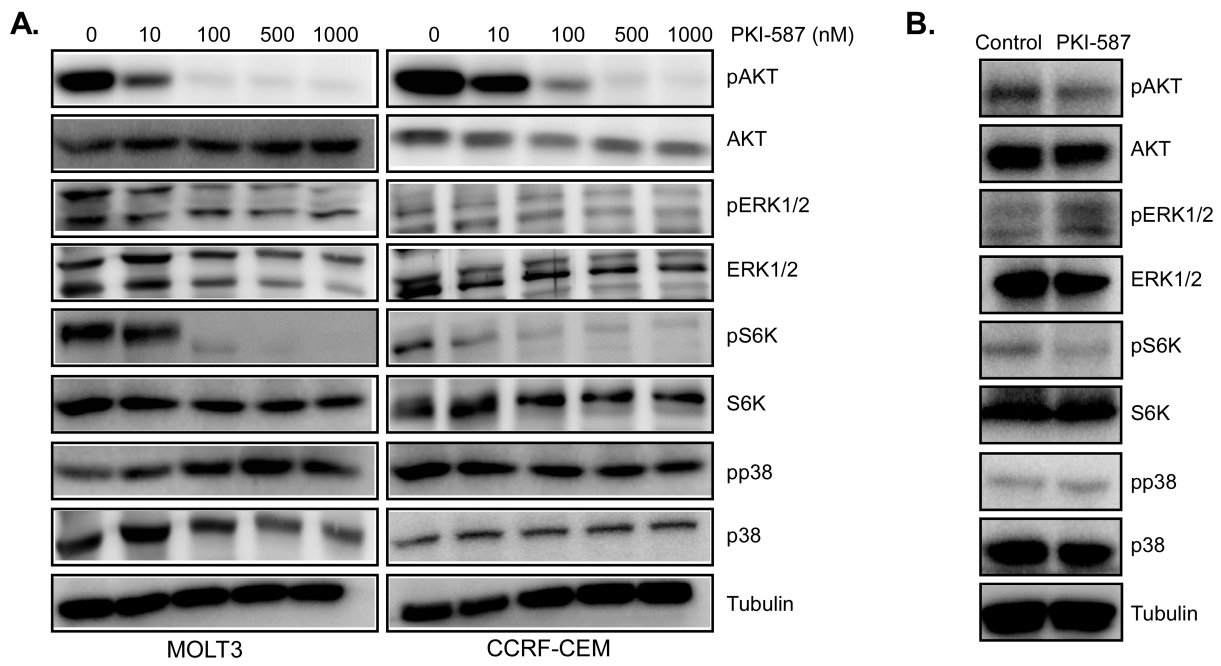


Figure 7